air

MDPI

Technical Note

FDS and AERMOD Simulations Towards Advancing Dispersion Modeling of Industrial Fires

Frank R. Freedman [1,2,*], Paolo Zannetti [1] and Adam K. Kochanski [2]

[1] EnviroComp Institute, Reno, NV 89511, USA; pzannetti@envirocomp.com
[2] Wildfire Interdisciplinary Research Center, San Jose State University, San Jose, CA 95192, USA; adam.kochanski@sjsu.edu
* Correspondence: frank.freedman@sjsu.edu

Abstract

We present FDS and AERMOD simulations of the Alaska Clean Seas (ACS) oil burn experiments to improve dispersion modeling of large, open-air fires relevant to industrial settings. We propose a method in which FDS smoke fields with available ground measurements are used to empirically calibrate AERMOD configured using volume sources to represent the fire source. FDS is first run for the three ACS experiments at high resolutions (~10 m) and verified against ground monitoring to provide detailed three-dimensional smoke fields. The fractional allocation of total fire emissions (weights, w_i) is then empirically specified for each volume source i so AERMOD smoke predictions fit both the ground level measurements and FDS simulations to acceptable accuracy. Runs for volumes at the surface (i = 1), 100 m AGL (i = 2) and 300 AGL (i = 3) and w_i = [0.01, 0.09, 0.9]–[0.04, 0.36, 0.6] accurately represent these data, suggesting this range as suitable for fire heat fluxes (~800–3000 kW/m^2), wind speeds (5–10 m/s) and PBL depths (300–500 m with and without capping temperature inversions) of the three ACS experimental burns. Further work exploring the applicability of this AERMOD setup to a broader range of conditions is ongoing.

Keywords: industrial fires; oil-pool fires; Gaussian dispersion modeling; fire modeling; Computational Fluid Dynamics; FDS; AERMOD

1. Introduction

Large outdoor fires at industrial warehouses or chemical storage facilities pose acute inhalation health risks due to the large amounts of smoke and possibly complex mix of species released. There is therefore a need for accurate and practical computational air dispersion models to estimate air concentration fields from such events, which can be used alongside available ground monitoring for health risk assessment or emergency response. Details on species emissions and ground-level concentration levels compared with acute health risk thresholds typical of industrial fires are presented in Griffiths et al. (2018), Griffiths et al. (2022) and Harper et al. (2026) [1–3].

Gaussian plume and puff air dispersion models such as AERMOD and CALPUFF [4,5] are routinely used for predicting hourly and longer-period averaged concentrations for a variety of typical industrial emission scenarios and source configurations. These models, however, are not designed for large open-air fires. A main reason is that the configuration and empirical database for their plume rise parameterizations are for industrial smokestack emissions, which are typically significantly less buoyant than large open-air fires. Also, penetrative convection parameterizations of plume entrainment across mixed-layer capping

Check for updates

Academic Editor: Ling Tim Wong

Received: 10 May 2026
Revised: 8 August 2026
Accepted: 10 August 2026
Published: 20 August 2026

Copyright: © 2026 by the authors. Licensee MDPI, Basel, Switzerland. This article is an open access article distributed under the terms and conditions of the Creative Commons Attribution (CC BY) license.

inversions are mainly for plumes with modest temperature elevations above ambient, rather than the higher temperature elevations often typical of fire plumes. Because of this, application of Gaussian models to fires is generally done empirically, assuming a user-preferred source type and values for source configuration parameters (e.g., stack exit temperature, stack exit velocity, and stack diameter) chosen so that the model matches in some way a pre-known state. This is the standard application approach for flares, in which a point source configuration is chosen with effective stack diameter calculated assuming an exit temperature of 1273 K and exit velocity of 20 m/s so the source heat flux matches a measured or assumed value of flare heat flux [6]. Similarly, Pratt et al. (2020) applied AERMOD to large oil pool fires from Deepwater Horizon by choosing a point source configuration with source parameters assigned so that modeled plume heights matched photographic and video evidence [7].

A more physically based modeling approach is Computational Fluid Dynamics (CFD). CFD models numerically integrate the underlying three-dimensional unsteady Navier–Stokes equations at spatial resolutions of fine-scale turbulent flow and buoyancy. When applied to fires, CFD models therefore allow better representation of plume rise and dispersion without the need for plume rise parameterizations. The drawback of CFD is the much higher computational cost compared to Gaussian models. The Fire Dynamics Simulator (FDS), developed by the U.S. National Institute of Standards and Technology (NIST), is a current publicly available CFD model designed and commonly used for simulating fires, both for indoor and outdoor situations [8].

NIST published several reports in the 1990s on measurements and modeling of smoke from open-sea oil fire experiments ([9–11], and references therein). Among the topics presented was ALOFT, a predecessor CFD model to FDS based on a two-dimensional (y-z, prescribed streamwise wind along x) version of the unsteady Navier–Stokes equations. The authors assessed ALOFT-predicted downwind smoke concentrations from experimental oil pool fires during the Alaska Clean Seas (ACS) campaign of September 1994. Simulations by ALOFT compared well with the experimental data within the range of uncertainty. Later, ALOFT was applied by Daly and Zannetti [12] to an industrial warehouse fire with satisfactory results. ALOFT, however, is no longer supported by NIST or publicly available.

Given this background, we present in this technical note modeling of the ACS experiments using FDS and AERMOD to assess and propose improvements to dispersion modeling of large, open-air fires relevant to industrial and similar settings. Specifically, we propose a method in which FDS-simulated smoke fields with available ground measurements can be used to empirically calibrate AERMOD configured using volume sources to represent the fire source. By combining the models, the advanced physics and full 3-D output of CFD and computational efficiency of Gaussian models are leveraged. FDS is first run at high resolutions (~10 m) and verified against ground monitoring to provide a baseline detailed three-dimensional smoke field. AERMOD is then configured with volume sources through the depth of the boundary layer overlying the fire, with the fractional allocation of total fire emissions (weights w_i, where index i represents a specific volume source) specified for each volume source so that AERMOD smoke predictions fit both the ground level measurements and the FDS simulated three-dimensional smoke distribution to an acceptable accuracy. By choosing volume sources rather than a point source, the configuration bypasses the difficulties and uncertainties of applying a Gaussian model plume rise algorithm to fires, while also explicitly allocating fire plume mass through the boundary layer consistent with observed fire dispersion behavior.

We present here an application of this method to the ACS experiments using three volume sources in AERMOD, one based at the surface (i = 1), the second at 100 m AGL (i = 2), and the third at 300 m AGL (i = 3). Four sets of weights are tested:

$[w_1, w_2, w_3]$ = [0.01, 0.09, 0.90], [0.02, 0.18, 0.80], [0.03, 0.27, 0.70], and [0.04, 0.36, 0.60], which successively allocate increasing fractions of smoke plume mass at and below 100 m. As will be shown, modeling results for both FDS and AERMOD fit well the ACS measurements. This lends confidence in the ability of FDS individually and AERMOD empirically calibrated to simulate accurately large open-air fires, at least within the range of fire heat fluxes and background ambient meteorology of the ACS experiments simulated here. Further study will more solidly verify and qualify this, as well as examine applicability to more general situations.

2. Methodology

2.1. ACS Experiments

The ACS oil burn experiments [9–11] were carried out in September 1994 at the Fire Training Ground in Prudhoe Bay, Alaska, to study the feasibility of controlled burning of emulsified oil for open-sea oil spill remediation. Three experiments (ACS-1, ACS-2, and ACS-3) were initiated from confined oil pools approximately 9 m in diameter, yielding a burn area of 64 m^2. ACS-1 and ACS-3 burned emulsions of crude oil and salt water, whereas ACS-2 burned just crude oil. The heat release in Megawatts and smoke particulate matter emissions in kg/s were reported for each fire based on estimates of the amount of oil consumed and laboratory measurements of heats of combustion for a variety of crude oils. Each burn lasted approximately one hour. Twelve MIE Real-Time Aerosol Monitors measuring PM10, based on passive optical sensing of forward scattered (towards sensor) near-IR radiation, were placed on tripods one meter above the ground at various locations approximately downwind of the burn during each experiment. Time series plots of measured PM10 over the duration of the burns from each monitor, as well as the average over the measurement duration, are provided in [9].

We digitized the provided PM10 measurement data to compare with model simulations. In Appendix A, Figure A1 shows the digitized monitor locations and Table A1 the extracted average and five-minute maximum PM10 concentrations for each monitor. The five-minute maximums were estimated by us from visual inspection of the time series plots. Only measurements for ACS-1 and ACS-2 were used since the monitor locations for ACS-3 were too close to the fire to be reliable for model comparison.

Meteorological measurements from ground stations and tethered blimps were also reported in [9], which we used as inputs for our modeling. Inputs for fire source characterization in the modeling given below are also taken from [9].

2.2. FDS

Simulations of fire plume flow and smoke dispersion for ACS-1, ACS-2 and ACS-3 were made using FDS Version 6.10.1, documented in the FDS User's Guide [8], hereafter referred to as the User's Guide. FDS numerically solves the unsteady Navier–Stokes equations assuming a low Mach number, applying second-order time and space finite-difference methods on a rectilinear Cartesian grid. Our runs were made in the default LES mode, which uses the Deardorff sub-grid scale turbulence parameterization.

The computational domain in meters was X = 10,000 (x = 0 to 10,000), Y = 1800 (y = −900 to 900), and Z = 2400 (z = 0 to 2400), with a grid resolution of 10 m, corresponding to 43.2 million grid points, with the fire source at x = 1000, y = 0, and z = 0. Open boundary conditions at the lateral and top boundaries, and a no-slip boundary condition at the ground with a sand grain roughness of 0.4 m (equivalent to an aerodynamic roughness length of 0.01 m, see Section 16.3.4 of the User's Guide) were applied. The simulation duration was 9000 s (t = 0 to 9000) with the fire initiated at 1500 s and lasting through the remaining duration. Output smoke concentration fields were averaged over

the last half of the simulation period t = 4500 to 9000 to obtain estimated hourly averages, consistent with the averaging period of AERMOD. The last half of the simulation period was chosen to avoid initial transients at the early stages of the fire affecting the FDS plume averages.

Fire inputs for each simulation are given in Table 1, as taken from [9]. Fires were represented using the burner approach described in the User's Guide, Section 9.1. In our implementation, the input parameters HRRPUA and HEAT_OF_COMBUSTION, representing the fire heat release rate per unit area in kW/m^2 and heat of combustion in kJ/kg, respectively, were specified. HRRPUA was specified over a surface patch covering the 10-m computational grid cell with upper-right corner at (x, y) = (1000, 0). The parameter AREA_MULTIPLIER was in turn set to 0.64, which explicitly forces the model to scale the mass and energy fire fluxes to reflect the true 64 m^2 burning footprint across the 100 m^2 cell. The smoke release rate per unit area (kg/m^2 s) is then internally computed by FDS based on HRRPUA, HEAT_OF_COMBUSTION and a specified value of SOOT_YIELD, representing the smoke yield (g smoke per gram fuel consumed), which was set to 0.116.

Table 1. Heat release and smoke emission inputs for FDS simulations [1].

Run	Heat Release Rate (MW)	HRRPUA (kW/m^2) [2]	Smoke Release Rate (kg/s) [3,4]
ACS-1	55	859	0.15
ACS-2	186	2906	0.51
ACS-3	98	1531	0.27

[1] Derived from values taken from [9]. [2] HRRPUA = 1000 × (Heat Release Rate)/(Burn Area). Burn area = 64 m^2. [3] Smoke Release Rate = 1000 × (Smoke Yield) × (Heat Release Rate)/(Heat of Combustion). Heat of Combustion = 42,000 kJ/kg and Smoke Yield = 0.116 g/g. [4] Range of uncertainty estimated ±20%.

Radiative transfer was calculated using the LES default optically thick parameterization. We set a specified radiative fraction of 0.1, which operates in high-temperature grids in the fire combustion zone where the numerical grid is too coarse to resolve detailed flame conditions. See the User's Guide, Section 14.1.3, for further details.

Meteorology was input as described in Section 16.1 and 16.5 of the User's Guide, whereby wind velocity and temperature profiles are specified as initial conditions through the domain and held constant at the inflow boundary. The specified initial profiles for the three experiments are shown in Figure 1, constructed using measurements reported in [9]. Main distinguishing features are the faster winds near the surface in ACS-2, and the presence of capping temperature inversions in ACS-2 and ACS-3, whereas ACS-1 is adiabatic through the vertical domain. Wind direction is set to 270 degrees (positive X) in all three cases. A wind direction standard deviation ("sigma-theta") of 10 degrees for ACS-1 and 15 degrees for ACS-2 and ACS-3 was applied according to values reported in [9]. Sigma-theta is a measure of variability in wind direction, which is applied stochastically in time as a gradual wind direction variation as described in the User's Guide, Section 16.1.

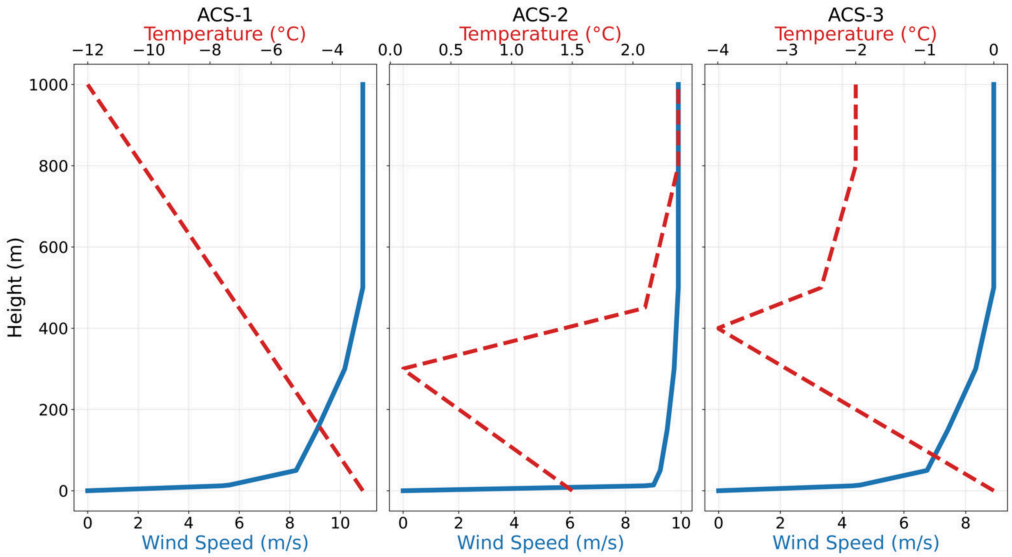


Figure 1. Input wind and temperature profiles to FDS simulation. Solid blue is wind speed profile; dashed-red is temperature profile.

The FDS runs were made on a computer cluster at the San Jose State University Wildfire Interdisciplinary Research Center. The cluster integrates multiple Grace Hopper compute nodes (GH200), each with 72 Grace ARM CPU cores, one H100 NVIDIA GPU, and 480 GB of RAM per node of shared memory using NDR400 InfiniBand, providing up to 400 Gb/s bandwidth between nodes. The runs utilized 144 processors across two nodes, assigning to each processor one of 144 equally sized meshes across the physical simulation domain. The ACS-1 and ACS-3 runs took approximately 24 h of clock time to complete, and the ACS-2 run took around 36 h to complete, with full use of cluster resources. The GPUs available on each node were not used.

The FDS input files for the ACS-1, ACS-2 and ACS-3 10 m resolution simulations described above are provided in the Supplementary Materials. FDS simulations were also carried out at 20 m horizontal resolution, which, while similar in main respects to the 10 m simulations, had higher plume diffusion likely due to less effective fine-scale flow resolution than 10 m. The 10 m resolution was thus judged as an upper-bound grid spacing that works within the resource limits of our cluster for full-domain runs. The presented FDS results are thus subject to uncertainty due to grid resolution, especially near the fire source where higher resolution would likely affect results. A set of 5 m resolution runs within a limited region around the fire are planned to further explore this issue and quantify uncertainty due to grid resolution.

We also performed FDS runs assuming no capping inversions in ACS-2 and ACS-3, and varying sigma-theta about the base values above. These contributed to our understanding and interpretation of the base simulation results.

2.3. AERMOD

The U.S. EPA AERMOD model Version 24142 was used to simulate smoke dispersion for the three experiments [13]. AERMOD is a Gaussian steady-state plume model, calculating individual plume concentration estimates at user-specified locations ("receptors") based on the analytical Gaussian plume equation as a function of hourly meteorological inputs. Emission sources can be configured as point, area, volume, or line, with associated parameters describing source location and geometry, emission rates, and, in the case of point sources, stack temperature and stack exit velocity.

A single hourly run of AERMOD was performed for each ACS-1, ACS-2, and ACS-3 since the experiments each lasted about an hour. A three-dimensional receptor grid of 50 m starting at the surface (z = 0) was specified, covering the horizontal extent of the FDS domain. Meteorological inputs, comprising surface wind speed (WSPD), friction velocity (USTAR), surface heat flux (HFLX) and mixed-layer height (PBLH), presented in Table 2, are based on reported values in [9]. HFLX is set to zero for all three cases to be consistent with the near-adiabatic temperature profiles (neutral stratification) in the lower boundary layer in all three cases (Figure 1). USTAR is computed from WSPD using the standard logarithmic profile relationship assuming a ten-meter reference height and a roughness length of 0.01 m. PBLH is set according to flight measurements of plume depths for ACS-1, and the base of the elevated temperature inversion for ACS-2 and ACS-3 (Figure 1).

Table 2. AERMOD meteorological inputs for each simulation.

Parameter	ACS-1	ACS-2	ACS-3
WSPD (m/s)	5.5	9.0	4.5
USTAR (m/s)	0.328	0.537	0.269
HFLX (W/m^2)	0	0	0
PBLH (m)	565	300	450

As described in the Introduction, we propose for AERMOD an empirical method for representing smoke emissions from fire sources using a series of volume sources spread through the boundary layer column overlying the fire. Specifically, weights (w_i) defined as the fraction of total fire smoke emissions allocated to volume source i are user inputs determined empirically. This can be from a priori analysis or directly for the case being modeled if data are available. The AERMOD smoke concentrations for the individual volume sources are then added to give the total concentration. In AERMOD, volume sources disperse according to ambient meteorological conditions absent the effects of plume rise and penetrative convection incorporated in point source algorithms. The use of volume sources, therefore, bypasses uncertainties in applying these point source algorithms to fires, for which the underlying parameterizations are not designed.

We utilize the ground PM10 measurements from the ACS experiments with the FDS simulated three-dimensional smoke fields to empirically determine the fractional emission weights. The purpose here is to introduce this AERMOD modeling approach as a demonstration, and therefore we do not propose nor apply at this time a formal quantitative method to fit these ACS and FDS data to the AERMOD concentrations, for example based on regression, cross-validation, bootstrapping, or other statistical methods. Instead, we rely on visual, qualitative inspection of model vs. measurements plots to justify a range of plausible weights that produce a reasonable fit. More formal, quantitative methods involving statistical analysis, of course, would be appropriate or required in practice for a particular application, which can be developed at that time depending on ground monitoring data availability and project goals.

For this demonstration, we ran AERMOD for each ACS experiment utilizing three volume sources: one at the surface (i = 1), a second at 100 m AGL (i = 2), and a third at 300 m AGL (i = 3). Initial sigma-y and initial sigma-z for each were set to 2.326 m (corresponding to volumes 10 m on a side). Four sets (S1, S2, S3 and S4) of weights were applied, which

all reasonably fit the measured data and FDS while also exhibiting important differences suggesting certain set members as "best" for each experimental case:

$$\begin{aligned} \text{Sn} &= [w_1, w_2, w_3], \text{ n} = 1 \text{ to } 4 \\ \text{S1} &= [0.01, 0.09, 0.90], \\ \text{S2} &= [0.02, 0.18, 0.80], \\ \text{S3} &= [0.03, 0.27, 0.70], \\ \text{S4} &= [0.04, 0.36, 0.60]. \end{aligned} \quad (1)$$

As seen, the sets are distinguished by the amount of smoke emissions allocated within 100 m (w_1 plus w_2), ranging from 0.1 to 0.4 from S1 to S4. These points are further discussed in the next section when examining the modeling results.

The AERMOD input files for each ACS run are provided in the Supplementary Materials.

3. Results

3.1. FDS

Figure 2 shows the downwind and vertical distributions of FDS simulated smoke concentrations along y = 0 averaged over t = 4500 to t = 9000 s for each experiment, shown as X-Z cross-sections across the entire domain (left panels) and vertical profiles of normalized concentrations by emission rate ($\mu g/m^3$ per g/s) at specific downwind distances x = 5000, 7500 and 10,000 (right panels). Plume lofting due to fire-induced buoyancy is evident, with plume centerline heights leveling off at around 200 m for ACS-1 and 300 m for ACS-2 and ACS-3. The NIST references [9–11] report plume depths (as distinct from centerline heights) from airplane recordings during ACS-1 between 550 and 600 m, and around 400 m for ACS-2. The depths of the simulated plume mass reasonably agree with these values. The ACS-2 and ACS-3 plumes level off just below the inversion base with a portion penetrating the inversion itself. As a result, relatively less plume mass reaches the surface in these cases compared to ACS-1, which is evident in the lower normalized values at the surface for ACS-2 and ACS-3 (just less than 0.1) than for ACS-1 (around 0.2). The higher plume heights induced by the larger fire heat flux in ACS-2 and ACS-3 compared to ACS-1 also contribute to this.

Figure 3 shows X-Y cross-sections of FDS-simulated smoke concentration at the surface (z = 0 m) averaged over t = 4500 to t = 9000 s for ACS-1 and ACS-2, along with the measured average (left of slash) and estimated five-minute maximum (right of slash) PM10. The simulated spatial patterns, while roughly aligned with and broadly symmetric about the theoretical westerly (left-to-right across the graphic) plume centerline, are complex and irregular. This is due to the highly unsteady fire plume behavior, associated with intermittent downmixing of plume mass to the surface at different surface positions over time. After time-averaging, this leads to average plumes being irregularly shaped and not necessarily along the theoretical westerly centerline. The plume unsteadiness can be seen from the time plots of the observations in [9] and in those from the simulations, which are presented in the Supplementary Materials, visually exhibiting similar characteristics in terms of concentration variations, frequency of peaks, and longer periods of low values. Overall, however, the simulated average pattern exhibits the expected decrease in surface concentration downwind and laterally away from the centerline. Comparing with observations, the simulated surface plume concentrations generally lie in value between the measured average and the five-minute maximums. Pointwise mismatches are largely due to the unsteadiness, a particular example being close to the fire source for ACS-2 where a slight southwesterly orientation of the simulated fire plume leads to the areas of simulated and measured peak concentrations to be misaligned.

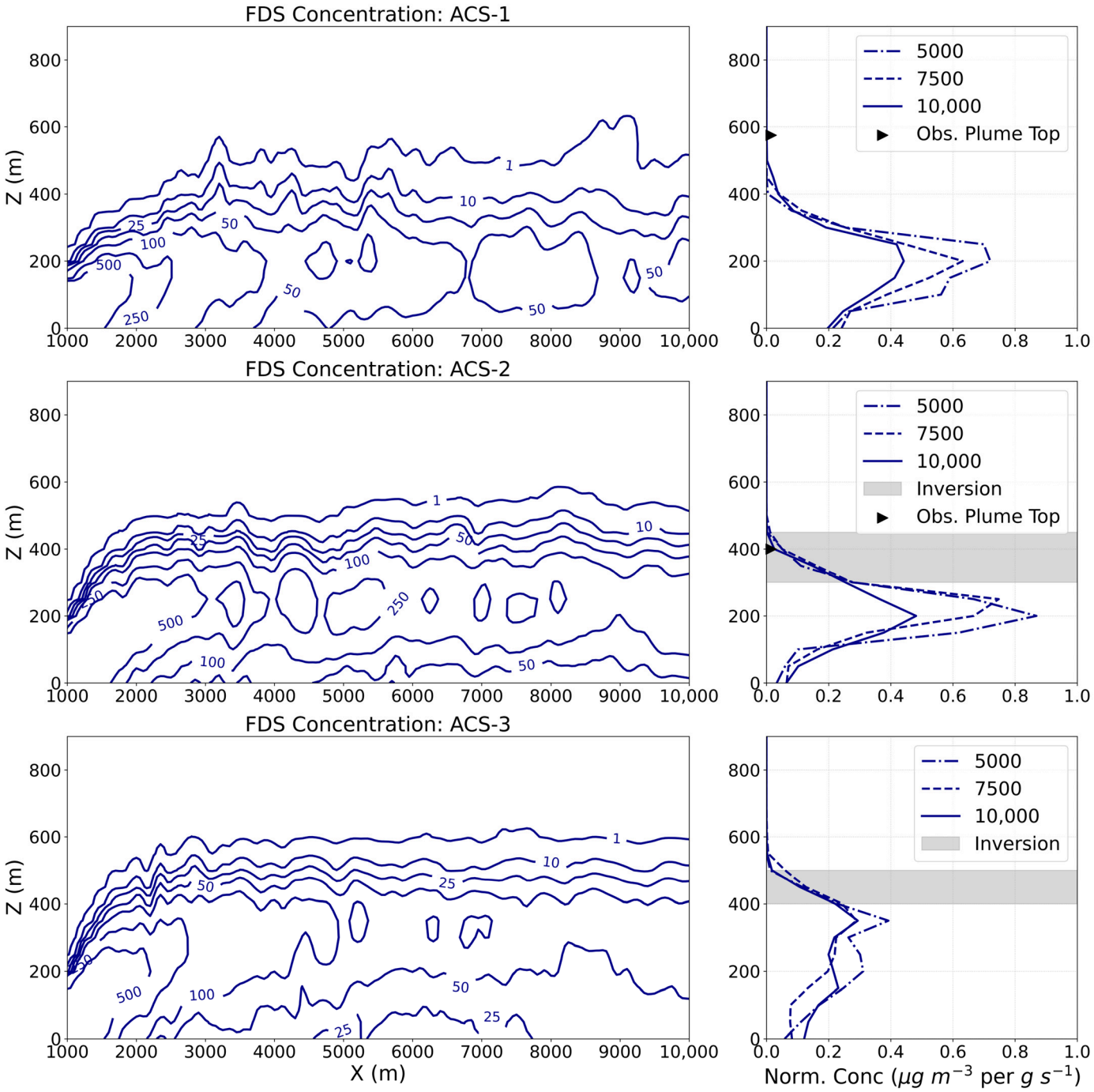


Figure 2. (**Left**) X-Z cross-sections of FDS simulated smoke concentration (μg/m^3) at y = 0 relative to the release point at origin (x = 1000, z = 0); (**Right**) Vertical profiles of normalized concentration by emission rate (μg/m^3 per g/s) at x = 5000, 7500 and 10,000. Plotted results are averages over the simulation period t = 4500 to t = 9000 s; (**top**) ACS-1, (**middle**) ACS-2, (**bottom**) ACS-3. Contour lines on the cross-sections are 500, 250, 100, 50, 10 and 1 μg/m^3. Gray banding on the right panels for ACS-2 and ACS-3 spans inversion layer depths depicted in Figure 1. Black triangles on the right panels for ACS-1 and ACS-2 are flight-track observed plume tops reported in [11].

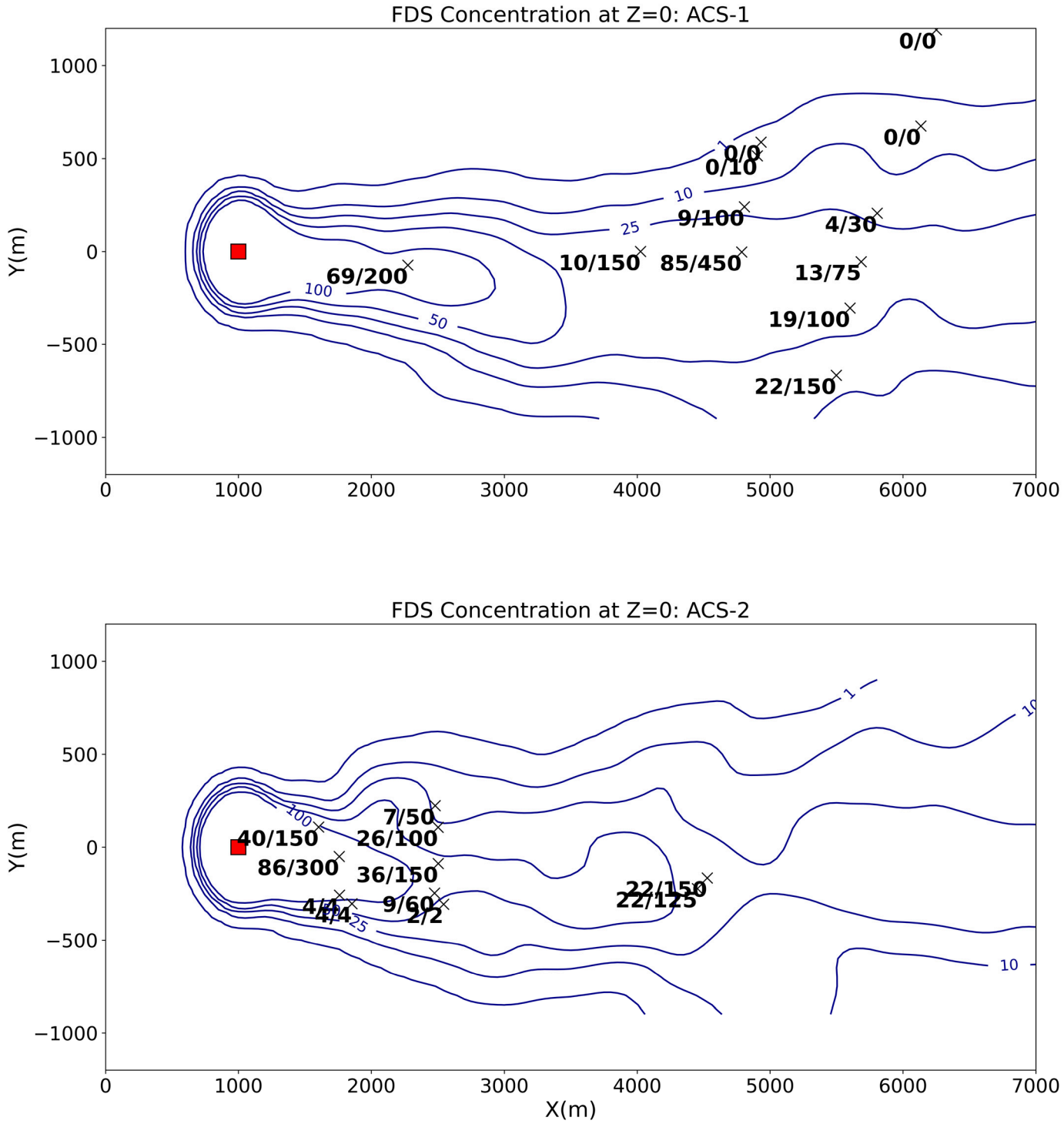


Figure 3. X-Y cross-sections of FDS simulated smoke concentration (μg/m^3) in the lowest model layer (z = 0–10 m) averaged over the period t = 4500 s to t = 9000 s; (**top**) ACS-1, (**bottom**) ACS-2. Contour lines are 100, 50, 25, 10 and 1 μg/m^3. Also plotted are concentration measurements taken during the experiments; '×' is the location of the measurement, the number left of the slash is the average and the number right of the slash is the estimated five-minute maximum. The red square is the location of the fire (x = 1000, y = 0, z = 0).

Additional details on FDS model versus measurement comparison for ACS-1 and ACS-2 are provided in Appendix A. Table A1 lists the modeled and measured surface concentrations at each monitor site along with basic statistics averaged over all sites. A scatterplot of the sorted and paired model and measured highest-to-lowest average

concentrations across monitors ("Q-Q" plot) is shown in Figure A2. The comparisons indicate broad factor-of-two agreement of the average concentrations. The main exception is for sites close to the fire (RAM-2, RAM-3, and RAM-4) for ACS-2, where, as mentioned above, a minor discrepancy in plume direction causes big mismatches.

3.2. AERMOD

As described in Section 2.3, AERMOD was configured with volume sources at the surface, 100 m and 300 m AGL. Runs with weights (w_i, i = 1, 2, 3) allocating the fraction of total fire smoke emissions across the three sources were carried out for four sets (S1, S2, S3, and S4), as defined in Equation (1). Concentration contributions from each source are added to give the total predicted concentration.

Figure 4 presents the predicted AERMOD surface concentrations as a function of distance from the fire at the plume centerline (y = 0) compared with the FDS and monitor data for the three experiments. The AERMOD surface concentrations increase at all distances from S1 to S4, consistent with the increasing emissions allocated to the lower elevated volumes (surface and 100 m) from 10% (S1) to 40% (S4). Each set broadly produces a reasonably good match to the data. In particular, the AERMOD predictions all generally lie between measured site mean and maximum concentrations. This gives support for the ranges defining the set emission allocations w_1 = 0.01–0.04, w_2 = 0.09–0.36, w_3 = 0.6–0.9 as generally appropriate to produce conservative hourly average surface concentration estimates for the experimental fire plumes. On the plot, we indicate by the solid-bold line sets S4 for ACS-1, S2 for ACS-2, and S2 for ACS-3 as "Main", which for the sake of demonstration we assign as "best match" to guide further examination below.

Figure 5 shows the AERMOD vertical cross sections along y = 0 for the Main sets, plotted as in Figure 2, as shown before for FDS. Comparing with Figure 2, the AERMOD Main sets match well the vertical plume mass variation between the surface and aloft in the FDS plumes. For ACS-1, normalized profiles capture the main basic features of a relatively more open plume compared with ACS-2 and AC3-3 (the AERMOD ACS-1 version slightly more open than FDS), with surface normalized values matching well the value of 0.2 found as well for FDS. The more concentrated plume aloft of ACS-2 and ACS-3 is also particularly well captured, with normalized profiles at the surface of 0.1 consistent between the models. As a sensitivity comparison, we plot in Figure 6 the sets that differ most from "Main" for each experiment: S1 for ACS-1 and S4 for ACS-2, and S4 for ACS-3. In each case, the vertical profile match to FDS is less accurate; in particular, S1 for ACS-1 has an overly concentrated elevated plume and lower normalized surface concentration, and the S4 plumes for ACS-2 and ACS-3 are too open. This shows that while all weight sets within the range may be deemed equally good (say within measurement uncertainty) if only looking at surface concentrations (Figure 4), using FDS to discern details of the match with respect to full plume vertical structure can identify weights that perform more optimally.

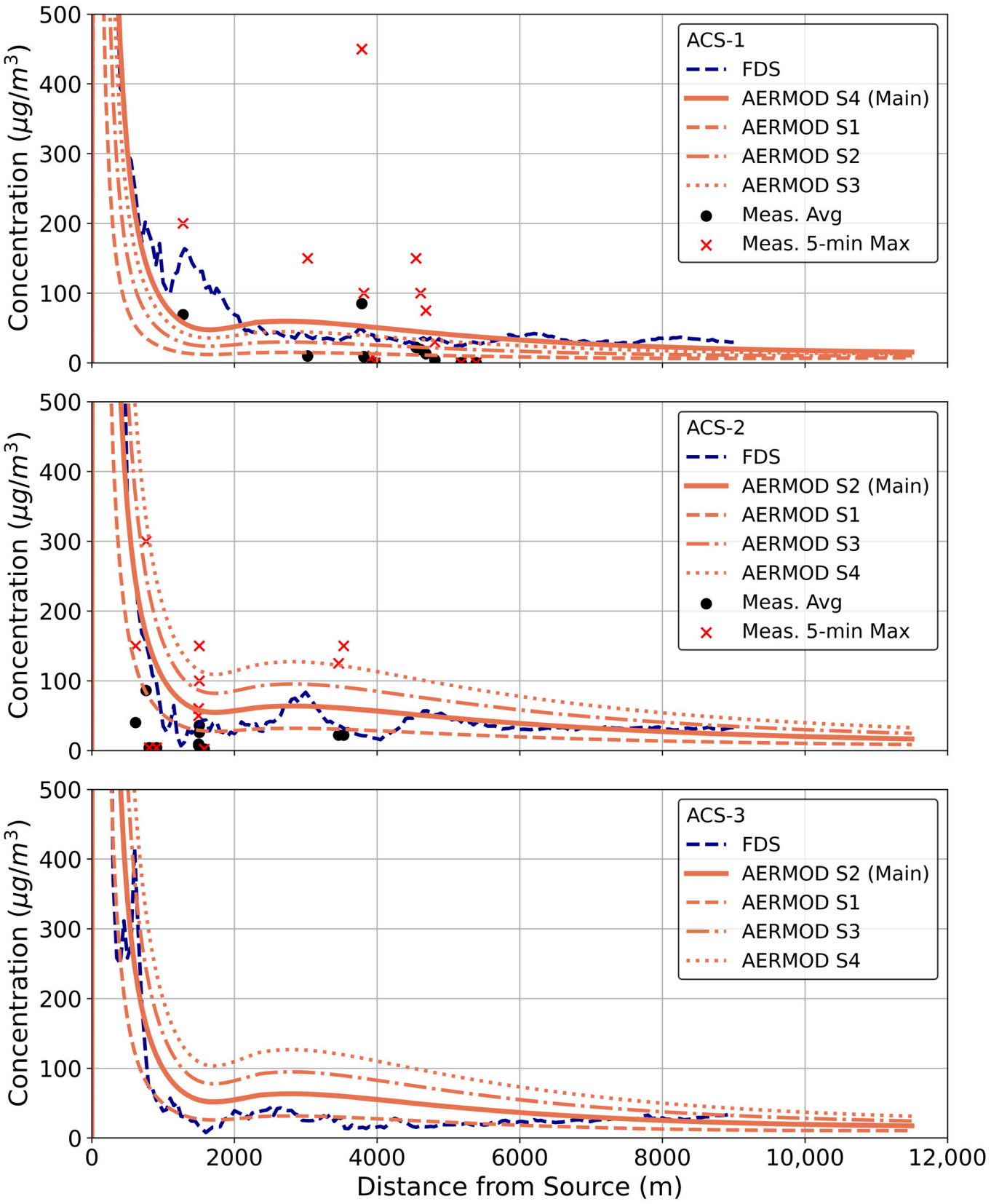


Figure 4. AERMOD surface concentrations (z = 0) as a function of distance from the fire at the centerline (y = 0) compared with FDS simulations in the lowest model layer (0–10 m) and monitor data for the three ACS experiments. AERMOD results are presented for four sets (S1, S2, S3 and S4) of emission weights w_i, defined by Equation (1). A main case giving a representative "best match" is identified for further focus, indicated by the solid thicker line.

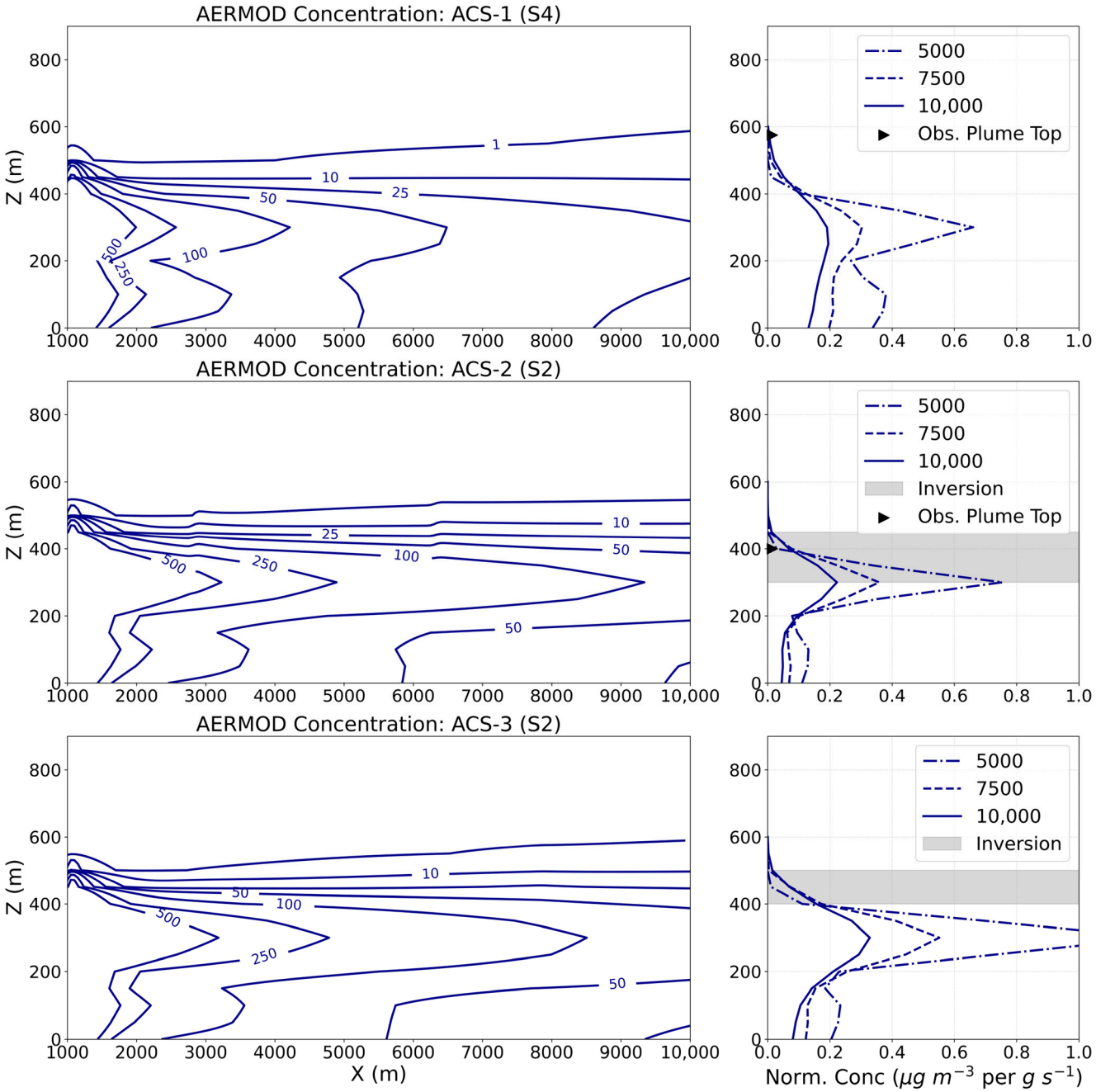


Figure 5. As Figure 2, but for AERMOD simulations: (**top**) ACS-1 Set 4, (**middle**) ACS-2 Set S2, (**bottom**) ACS-3 Set S2.

Figure 7 shows the AERMOD X-Y cross-sections of simulated surface concentration patterns for the Main ACS-1 S4 and ACS-2 S2 runs plotted atop measurements. An excellent match to observations can be seen. Contour lines are smoother than those of FDS due to the steady-state plume model design of AERMOD, which enforces lateral symmetry about the downwind axis. Complexities associated with unsteady dispersion of the actual fires and directly accounted for by FDS are therefore not simulated by AERMOD, which instead represents a theoretical average steady-state.

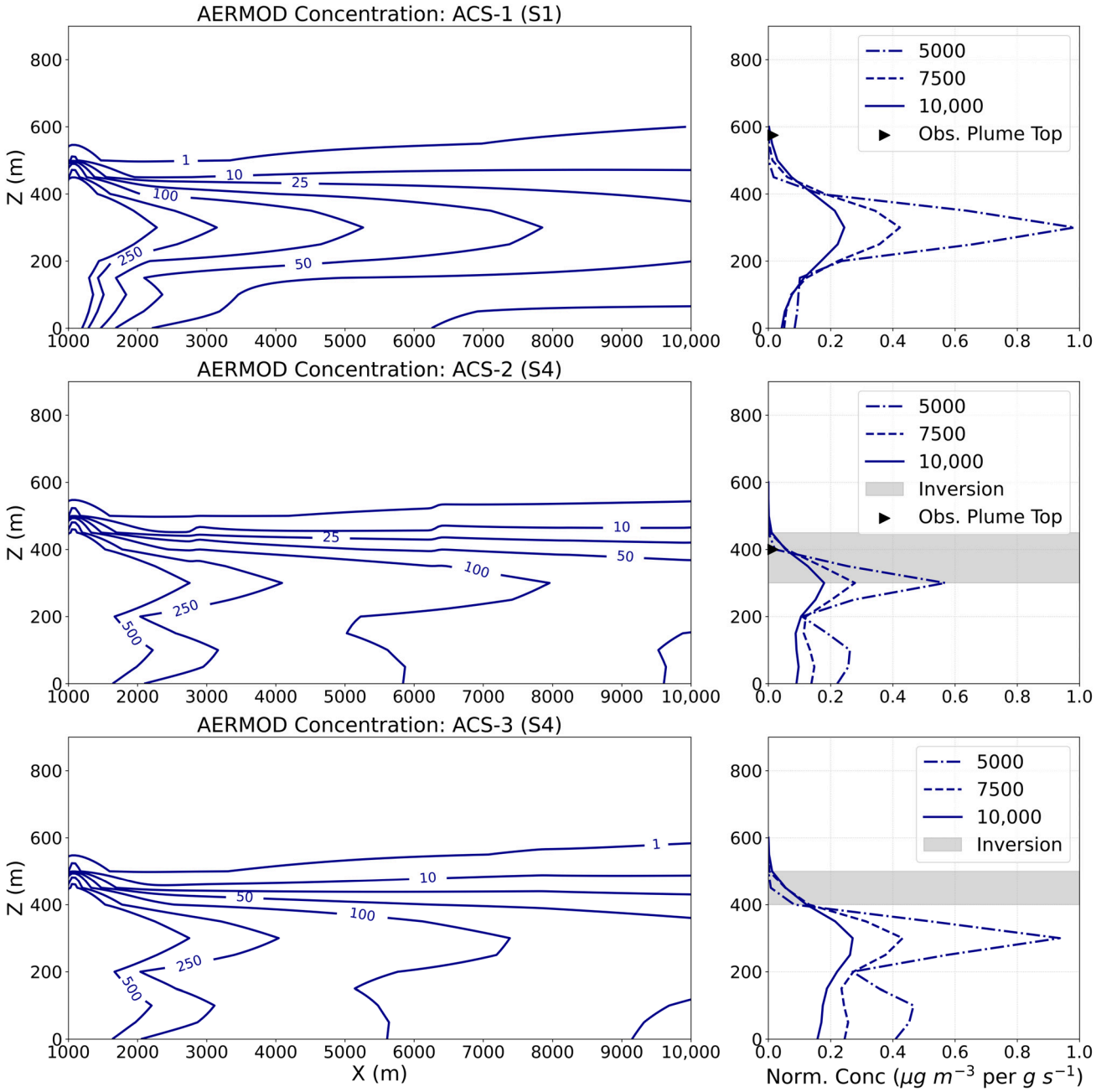


Figure 6. As Figure 5, but for AERMOD simulations: (**top**) ACS-1 Set 1, (**middle**) ACS-2 Set S4, (**bottom**) ACS-3 Set S4.

Table A1 lists for ACS-1 and ACS-2 the AERMOD modeled and measured surface concentrations for the Main sets at each monitor site along with basic statistics averaged over all sites. A scatterplot of the sorted and paired model and measured highest-to-lowest concentrations across monitors ("Q-Q" plot) is shown in Figure A2. The comparisons indicate broad factor-of-two agreement among average and sorted concentrations.

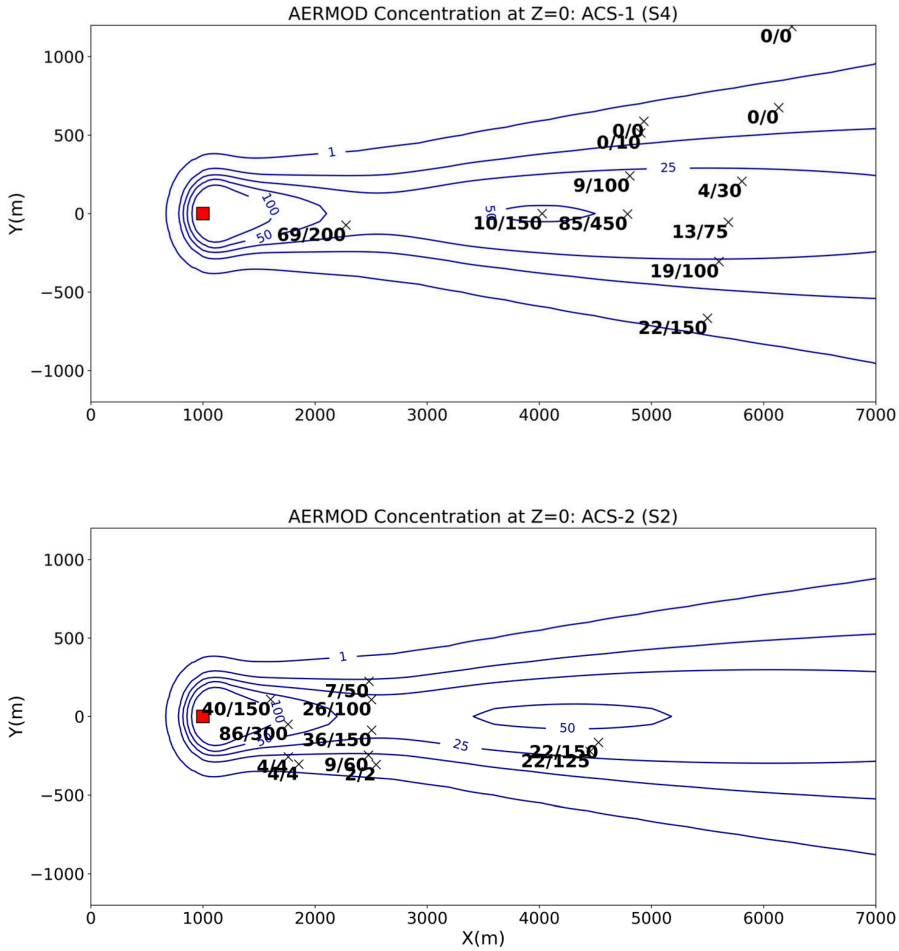


Figure 7. As in Figure 3, but for AERMOD surface concentrations (z = 0): (**top**) ACS-1 Set S4, (**bottom**) ACS-2 Set S2.

4. Conclusions

FDS and empirically calibrated AERMOD simulations carried out in this study produced reasonably accurate measurements of smoke PM10 concentrations during the ACS oil-pool fire experiments. This provides confidence in the ability of current publicly available CFD and Gaussian models to simulate large industrial and similar fires, at least for conditions similar to ACS.

Some main conclusions drawn from this, pointing to directions for future work, are as follows:

FDS: The pool fire ("burner") approach in FDS, where fire heat flux, heat of combustion, and species emission factors are prescribed inputs, appears suitable for large open-air fires despite the relative simplicity of the approach compared to more complex models of combustion and pyrolysis. This is likely the best approach for simulating real-world open-air industrial fires with FDS, given the difficulty of characterizing the details of combustion materials and processes in real-world situations. The 10 m resolution used for our simulations appears adequate to resolve the fire plume; however, uncertainties, especially near the fire source, are noted since 5 m runs were not carried out at this time due to computer cluster limitations. Thus, in summary, while computationally expensive, FDS appears able to effectively capture the complexity, lateral meandering, and unsteadiness of large-scale fire circulations and dispersion, and therefore is an effective tool for obtaining a high-fidelity simulation of large outdoor fire plumes not possible with simpler analytical steady-state Gaussian models. If a theoretical steady-state is desired, similar to axisymmet-

ric plumes produced by the Gaussian models, a possible approach is to run ensembles of FDS simulations with slight variations in input variables and then average the simulated concentrations over the ensemble. We are currently testing this approach as future work.

AERMOD: Our proposed empirical approach is to configure AERMOD with volume sources in the boundary layer overlying the fire source and allocate fractions of total emissions ("weights", w_i) to the sources so that resulting AERMOD simulations reproduce to reasonable accuracy ground measurements and FDS simulations. The success of the specific setup applied here, three volume sources at the surface, 100 m AGL and 300 AGL, demonstrates practical feasibility of the approach, and broadly suggests weights in the range w_i = [0.01, 0.09, 0.9]–[0.04, 0.36, 0.6], equating to 10–40% allocation of fire smoke plume mass within the lowest 100 m, as accurate to represent the fire plumes characteristic of the fire fluxes and meteorological conditions of the three ACS experimental burns; fire heat fluxes ~800–3000 kW/m^2, wind speeds 5–10 m/s, PBL depths 300–500 m with and without capping temperature inversion. The detailed vertical profile simulation data provided by FDS were useful to identify a set within this range that gave best results for each experiment. This points to the important role of the FDS data in the empirical process, especially for vertical profile information beyond what ground observations and simple photographs alone can provide.

Implications: Our hypothesis is that this empirical approach will ultimately be generally applicable for simulating industrial fires with AERMOD without extensive trial-and-error parameter readjustment. To meet the goal of determining this, work is needed to investigate the generalizability of the approach beyond the range of conditions investigated here. The main physical parameters affecting fire dynamics are the fire heat flux, background wind speed, and atmospheric stability, including the presence or absence of capping inversion layers affecting PBL depth. We are currently exploring datasets and designing further FDS simulations that fill out this parameter space, which will then provide a baseline empirical dataset to develop more precise and likely expanded ranges of weights for AERMOD to accurately model a broader range of fires using this approach.

Supplementary Materials: The following supporting information can be downloaded at: https://www.mdpi.com/article/10.3390/air4030019/s1: File S1: Input files for FDS and AERMOD simulations and File S2: Time plots (every five-minute simulation time) of FDS simulated concentrations at eachmonitoring station location for ACS-1 and ACS-2.

Author Contributions: Conceptualization, F.R.F. and P.Z.; methodology, F.R.F., P.Z. and A.K.K.; validation, F.R.F.; formal analysis, F.R.F.; investigation, F.R.F.; resources, A.K.K.; data curation, F.R.F.; writing—original draft preparation, F.R.F., P.Z. and A.K.K.; writing—review and editing, F.R.F., P.Z. and A.K.K.; visualization, F.R.F.; project administration, F.R.F.; funding acquisition, P.Z. All authors have read and agreed to the published version of the manuscript.

Funding: This research was partially funded by the EnviroComp Institute: EIN 73-1651418, U.S. Forest Service: USFS project 22-CR-11221633-027, and National Aeronautics and Space Administration: NASA grants 80NSSC23K1344 and 80NSSC25K7276.

Institutional Review Board Statement: Not applicable.

Informed Consent Statement: Not applicable.

Data Availability Statement: Input files to reproduce the FDS and AERMOD model output presented in this paper are provided in the Supplementary Materials. The original contributions presented in this study are included in the article and Supplementary Materials. Further inquiries can be directed to the corresponding author.

Use of Artificial Intelligence: Used to write Python scripts for post-processing model simulation results and generating figures. Python version 3.11.7 was used. The authors have reviewed and edited the output and take full responsibility for the content of this publication.

Acknowledgments: The authors acknowledge the support of the San Jose State University Wildfire Interdisciplinary Research Center for making its research computer cluster available and providing technical support.

Conflicts of Interest: Authors Frank Freedman and Paolo Zannetti were employed by the Enviro-Comp Institute. The remaining author declares that the research was conducted in the absence of any commercial or financial relationships that could be construed as a potential conflict of interest. The authors declare that this study received funding from the EnviroComp Institute. The funder was not involved in the study design, collection, analysis, interpretation of data, the writing of this article or the decision to submit it for publication.

Appendix A

Table A1. FDS and AERMOD concentrations versus measurements for (**a**) ACS-1 and (**b**) ACS-2. FDS results are averages over the simulation period t = 4500 s to t = 9000 s. FDS model maximums are from values sampled every 300 s over this period (see time plots provided in Supplementary Materials). AERMOD results are for set S4 (ACS-1) and set S2 (ACS-2) simulations, as described in Section 2.3. Measurements obtained from Appendix of [9], as described in Section 2.1. All concentrations in $\mu g/m^3$.

(**a**) **ACS-1**					
ID	**FDS (Avg)**	**FDS (Max)**	**AERMOD (S4)**	**Measured (Avg)**	**Measured (Max)**
RAM-1	47	193	53	85	450
RAM-2	18	157	28	9	100
RAM-3	1.6	25	1.9	0	0
RAM-4	12	128	2.2	22	150
RAM-5	28	103	24	19	100
RAM-6	36	122	43	13	75
RAM-7	22	99	33	4	30
RAM-8	3.0	46	2.5	0	0
RAM-9	2.9	45	4.9	0	10
RAM-10	0.01	0.05	0.2	0	0
RAM-11	110	414	50	69	200
RAM-12	37	137	59	10	150
AVG (Sites)	26	122	25	19	105
(**b**) **ACS-2**					
ID	**FDS (Avg)**	**FDS (Max)**	**AERMOD (S2)**	**Measured (Avg)**	**Measured (Max)**
RAM-1	32	296	32	40	150
RAM-2	197	1305	119	86	300
RAM-3	170	1389	0.14	4	4
RAM-4	36	315	0.10	4	4
RAM-5	11	114	7.5	7	50
RAM-6	39	353	34	26	100
RAM-7	38	185	34	36	150
RAM-8	40	384	2.5	9	60
RAM-9	13	146	0.78	2	2
RAM-11	39	117	45	22	150
RAM-12	39	140	35	22	125
AVG (Sites)	60	431	28	23	100

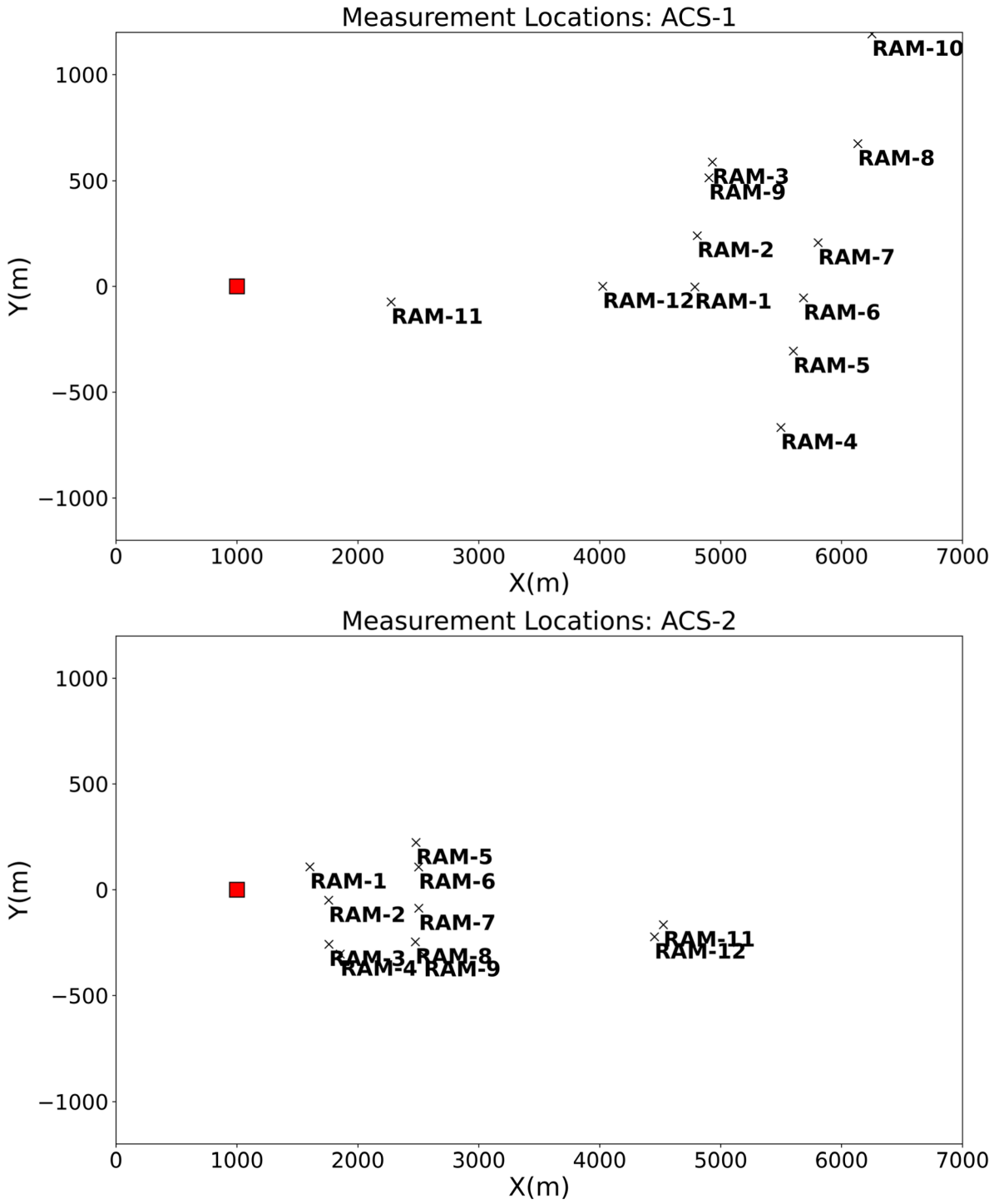


Figure A1. Locations of monitoring for the ACS-1 and AC2-2 experiments, as indicated by '×' The fire source location at x = 1000 and y = 0 is indicated with the red square. Downwind is oriented left to right across the graphic in both cases.

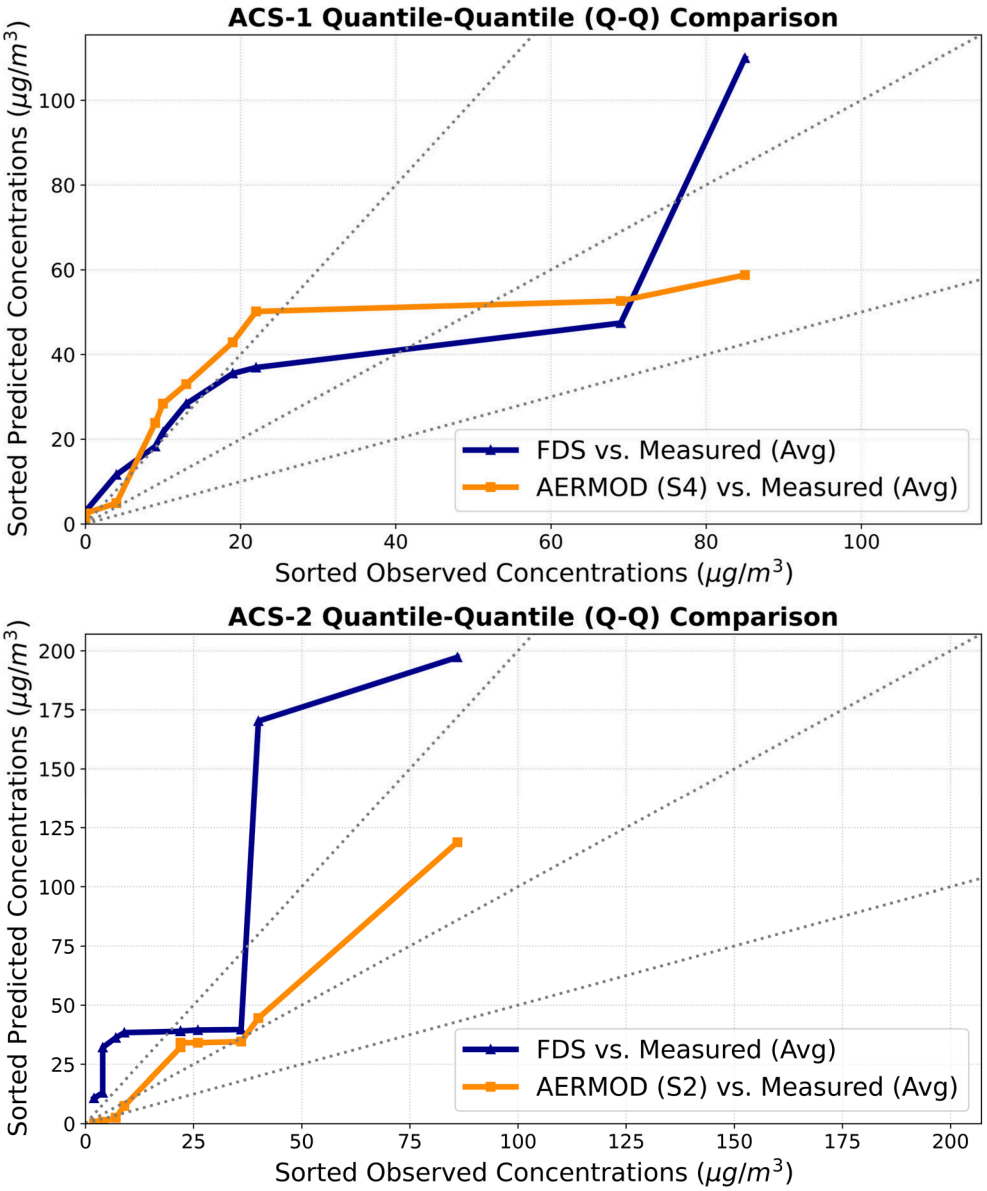


Figure A2. Sorted observed versus FDS and AERMOD modeled average surface concentrations ("Q-Q plots") for ACS-1 (**top**) and ACS-2 (**bottom**). Data taken from Table A1. Middle dotted line is one-to-one, lower and upper dotted lines are factor-of-two differences between model and monitor.

References

1. Griffiths, S.D.; Chappell, P.; Entwistle, J.A.; Kelly, F.A.; Deary, M.E. A study of particulate emissions during 23 major industrial fires: Implications for human health. *Environ. Int.* **2018**, *112*, 311–323. [CrossRef] [PubMed]
2. Griffiths, S.D.; Entwistle, J.A.; Kelly, F.A.; Deary, M.E. Characterising the ground level concentrations of harmful organic and inorganic substances released during major industrial fires, and implications for human health. *Environ. Int.* **2022**, *112*, 107152. [CrossRef] [PubMed]
3. Harper, C.A.; Arterburn, L.; Paredero, K.; El Asmar, R.; Stewart, M.L.; Tanner, D.J.; Roberts, J.M.; Orlando, J.J.; Sadighi, J.; Weber, R.J.; et al. Observations of the Gas Phase Composition of the 2024 BioLab Industrial Plume in the Atlanta Metropolitan Area. *Environ. Sci. Technol. Lett.* **2026**, *13*, 664–669. [CrossRef] [PubMed]
4. Cimorelli, A.J.; Perry, S.G.; Venkatram, A.; Weil, J.C.; Paine, R.J.; Wilson, R.B.; Lee, R.F.; Peters, W.D.; Brode, R.W. AERMOD: A dispersion model for industrial source applications. Part I: General model formulation and boundary layer characterization. *J. Appl. Meteorol.* **2005**, *44*, 682–693. [CrossRef]
5. Scire, J.S.; Strimaitis, D.G.; Yamartino, R.J. *A User's Guide for the CALPUFF Dispersion Model (Version 5)*; Earth Tech, Inc.: Concord, MA, USA, 2000; p. 521. Available online: https://calpuff.org/calpuff/download/CALPUFF_UsersGuide.pdf (accessed on 17 March 2026).

6. Zelensky, M.J.; Zelt, B.W. Pseudo-source parameters for flares: Derivation, implementation, and comparison. *J. Air Waste Manag. Assoc.* **2019**, *69*, 450–458. [CrossRef] [PubMed]
7. Pratt, G.C.; Stenzel, M.R.; Kwok, R.K.; Groth, C.P.; Banerjee, S.; Arnold, S.F.; Engel, L.S.; Sandler, D.P.; Stewart, P.A. Modeled Air Pollution from In Situ Burning and Flaring of Oil and Gas Released Following the Deepwater Horizon Disaster. *Ann. Work Expo. Health* **2022**, *66*, i172–i187. [CrossRef] [PubMed]
8. National Institute of Standards and Technology (NIST). FDS-SMV (Fire Dynamics Simulator and Smokeview). Available online: https://pages.nist.gov/fds-smv/ (accessed on 17 March 2026).
9. McGrattan, K.B.; Walton, W.D.; Putorti, A.D.; Twilley, W.H.; McElroy, J.; Evans, D.D. *Smoke Plume Trajectory from In Situ Burning of Crude Oil in Alaska: Field Experiments*; NISTIR 5764; National Institute of Standards and Technology: Gaithersburg, MD, USA, 1996. Available online: https://nvlpubs.nist.gov/nistpubs/Legacy/IR/nistir5764.pdf (accessed on 27 March 2026).
10. McGrattan, K.B.; Baum, H.R.; Rehm, R.G. Numerical simulation of smoke plumes from large oil fires. *Atmos. Environ.* **1996**, *30*, 4125–4136. [CrossRef]
11. Evans, D.D.; Mulholland, G.W.; Baum, H.R.; Walton, W.D.; McGrattan, K.B. In Situ Burning of Oil Spills. *J. Res. Natl. Inst. Stand. Technol.* **2001**, *106*, 231–278. [CrossRef] [PubMed]
12. Daly, A.; Zannetti, P.; Echekki, T. A Combination of Fire and Dispersion Modeling Techniques for Simulating a Warehouse Fire. *Int. J. Saf. Secur. Eng.* **2012**, *2*, 368–380. [CrossRef]
13. AERMOD Modeling System. Available online: https://www.epa.gov/scram/air-quality-dispersion-modeling-preferred-and-recommended-models#aermod. (accessed on 18 March 2026).

Disclaimer/Publisher's Note: The statements, opinions and data contained in all publications are solely those of the individual author(s) and contributor(s) and not of MDPI and/or the editor(s). MDPI and/or the editor(s) disclaim responsibility for any injury to people or property resulting from any ideas, methods, instructions or products referred to in the content.